

## Anti-jamming of Inverse Synthetic Aperture Radar based on Slope-varying Linear Frequency Modulation Signal

Zhu Yupeng, Wu Liang, Wang Hongqiang, and Li Xiang

*National University of Defense Technology, Changsha, Hunan 410073, China*

### ABSTRACT

Deceptive jamming technology against inverse synthetic aperture radar is matured now, which is meaningful in military application. But the research on anti-jamming technology for inverse synthetic aperture radar (ISAR) is still not a mature technology. Through the analysis on the theory of deceptive jamming technology against ISAR, a new method for anti-jamming against ISAR based on linear frequency modulation signal's frequency slope-varying is presented. The false target echo energy is suppressed due to frequency modulation slope mis-matching. Doppler domain averaging is adopted for improving the quality of the ISAR image, which helps automatic target recognition. Simulation result based on simulating data shows the validity of the new algorithm.

**Keywords:** Inverse synthetic aperture radar, deceptive jamming, anti-jamming, doppler blurring, doppler domain averaging, linear frequency modulator, automatic target recognition, ISAR, ATR

### 1. INTRODUCTION

Inverse synthetic aperture radar (ISAR) image is the projection of target scattering centre on the scan plane of radar. It can reflect two-dimensional equivalent electromagnetic scattering distribution and structure feature and which is an effective mean of radar target characteristic analysis and recognition.[1,2] With the increase in the development of microwave material and manufacturing technology and improvement of the theory of radar imaging, ISAR is successfully applied to target detection, perception, identification, and other military fields such as precision-guided weapons. US Naval AN/APS-147 radar with ISAR imaging and other multi-mode functions has been equipped with Sea Hawk SH-60R armed helicopter. ISAR in the Russian Sea Dragon submarine patrol system is able to image the ground and surface targets. Besides, US GBR-X has been used to detect ballistic target in favour of anti-missile system seeking and recognition. ISAR with high-resolution, all-day, all-weather and directly observational characteristics plays an important role in military field, which makes the active jamming to ISAR to be a new research area [3,4,6].

To realise suppression jamming, the jamming signal with high power makes the ISAR image distorted by destructing motion compensation or target range profile. The principle of deceptive interference is that radar signal is detected by jammer, transformed by a certain way, and transmitted back to ISAR, so it will receive the jamming and real target echo signals together. Jamming signal will be imaged as false target in ISAR image. To ISAR deceptive interference, studied done in the technology of digital

image synthesis (DIS) against chirp ISAR, concluded that the DIS combined with high-instantaneous-wideband digital RF memory (DRFM) can synthesise the jamming signal of false target [3]. Another study realised a deceptive jamming against ISAR in anti-missile system and studied the method by which the real-time echo signal of false ballistic targets is produced [4]. With the development of ISAR jamming technology, it is important to develop ISAR anti-jamming and strengthen the ISAR electromagnetic combating ability, but less research about ISAR anti-jamming is reported.

In this paper, to realise the active ISAR anti-jamming, a method of slope-varying LFM signal is proposed. To the cheater against ISAR, the key parameters of signal transmitted by ISAR must be first detected, and the false target signal is synthesised by DRFM and DIS. But ISAR can modulate some parameters of the transmitted signal actively and continually at the imaging stage and makes it difficult for the cheater to detect accurate and real-time parameters, so the false target signal will be suppressed so as to realise ISAR active anti-jamming .

### 2. PRINCIPLE OF ISAR DECEPTIVE JAMMING

The space target has different shapes and complex structure, usually consists of many scattering centres with different reflection coefficients and locations. Radar imaging is to display the location and echo intensity of each scattering centre correctly and reconstruct the feature of target structure for target electromagnetic characteristics analysis and recognition and so on. As long as parameters of signal transmitted by ISAR are detected, to realise deceptive

jamming against ISAR, the echo of false target is simulated and transmitted back to ISAR by antenna. Because of the same characteristics between false and real target echo signal, false target will also be displayed while the received signal is imaged, so the active deceptive jamming against ISAR is realised.

**2.1 Principle of ISAR Imaging**

Assume that the distribution of target reflection coefficient is  $\sigma(x,y)$ ,  $XOY$ , is the fixed coordinate system of target and

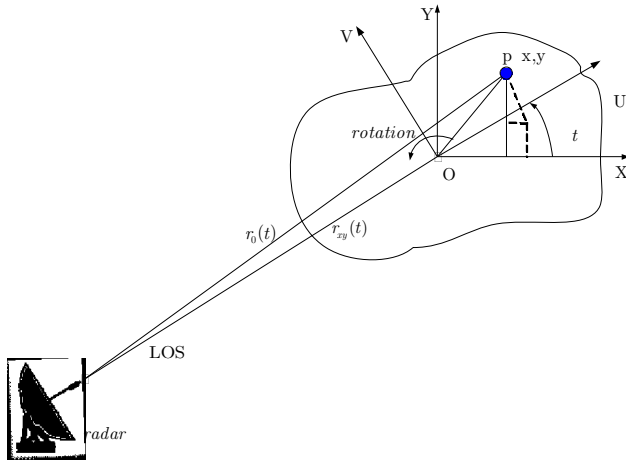


Figure 1. Geometry of ISAR imaging.

$UOV$  is a coordinate system from radar line of sight (RLOS), their origins coincide with target rotating centre. Suppose radar transmits LMF signal, the carrier frequency  $f_0$  is, the slope of frequency is  $\mu$ , the pulse duration is  $\tau$ , the intercepted pulse interval is  $T$ ,  $\hat{t}$  is the fast time from the transmitting time  $t_m = mT$ , is the slow time of each pulse,  $t = \hat{t} + mT$  is the full time, so the  $m$ -th pulse signal transmitted by ISAR is

$$s_t(\hat{t}, t_m) = \text{rect}\left[\frac{t - mT}{\tau}\right] e^{j2\pi[f_0 t + \frac{1}{2}\mu(t - mT)^2]} \quad (1)$$

where

$$\text{rect}[t] = \begin{cases} 1 & |t| \leq \frac{1}{2} \\ 0 & |t| > \frac{1}{2} \end{cases}$$

a target  $P(x,y)$  scatter at  $UOV$  is

$$\begin{cases} u = x \cos \theta + y \sin \theta \\ v = -x \sin \theta + y \cos \theta \end{cases} \quad (2)$$

At  $t_m$  moment, the distance between  $P(x,y)$  and radar phase centre is  $r_{xy}(t_m) \approx R_0(t_m) + u$ , the target echo can be expressed as

$$s_r(\hat{t}, t_m) = \iint_S \sigma(x,y) \text{rect}\left[\frac{\hat{t} - 2r_{xy}(t_m)/c}{\tau}\right] \exp\{j\pi[2f_0(t - \frac{2r_{xy}(t_m)}{c}) + \mu(\hat{t} - \frac{2r_{xy}(t_m)}{c})^2]\} dx dy \quad (3)$$

where  $S$  donates target region. The  $m$ -th pulse is delayed as reference signal, the Dechirp processing result of radar echo signal is arranged as

$$S_r(f, t_m) = e^{j\varphi_m(f)} e^{\varphi_0^m} \iint_S \sigma(x,y) e^{-j2\pi f \frac{2u}{c}} dx dy \quad (4)$$

where  $f = f_0 + \mu \hat{t}$ ,  $\tau_0(t_m) = \frac{2r_0(t_m)}{c}$

$$\varphi_m(f) = 2\pi f(\tau_s^m - \tau_0^m)$$

$$\varphi_0(f) = -\pi\mu(\tau_s^m - \tau_0^m)^2$$

At  $t_m$  moment, target rotation angle is  $\theta_m$ . Note that  $u = x \cos \theta + y \sin \theta$  and the target centre is assumed to be tracked accurately by motion compensation algorithm. So there is  $\tau_s^m = \tau_0^m$ , thus

$$S_r(f, t_m) = \iint_S \sigma(x,y) e^{-j2\pi f \frac{2(x \cos \theta_m + y \sin \theta_m)}{c}} dx dy \quad (5)$$

While the uniform rotation angular velocity is  $\Omega$  and rotation angular is relatively small,  $\cos \theta_m \approx 1$ ,  $\sin \theta_m \approx \theta_m \approx m\Omega T$ , so the Eqn (5) can be approximately expressed as

$$S_r(f, t_m) = \iint_S \sigma(x,y) e^{-j2\pi f \frac{2x}{c}} e^{-j2\pi f_0 \frac{2y}{c} m\Omega T} dx dy \quad (6)$$

The discrete Eqn (6) is

$$S_r(n, m) = \sum_i \sigma_i e^{-j2\pi f_n \frac{2x_i}{c}} e^{-j2\pi f_0 \frac{2y_i}{c} m\Omega T} \quad (7)$$

where the scatter intensity at the point  $(x_p, y_i)$  is  $\sigma(x_p, y_i)$ ,  $f_n = f_0 + \mu \hat{t}_n$  is the sampling point in the fast time domain,  $S_r(n, m)$  is discrete sampling echo signal at  $n$ -th slow time and  $n$ -th fast time.

**2.2 Principle of ISAR Deceptive Jamming**

It can be seen from the Eqn (7) that the target echo is the overlap of all scatters' echo signal. The distribution of each scatter along the range direction reflects the delayed modulation of transmitted signal, the distribution along the azimuth direction reflects the Doppler frequency modulation and the RCS reflects the variety of echo energy. To deceptive jamming, according to the distribution of false target reflection coefficient  $\sigma'(x_j, y_j)$  and rotation angle  $\theta_m$  that induces azimuth Doppler, the transmitted signal is transformed by amplitude modulation (AM), frequency modulation (FM) and time delay at given range units, and the overlap of simulated signal at each range unit will produce all of the false target echo signal. Specifically, Assume that the coordinates of jammer on the target are  $(x_o, y_o)$  at the range and azimuth direction, the scattering intensity is  $\sigma_o$ , so the under-mixed-frequency result of echo signal received by ISAR at this location is

$$s_o(\hat{t}, t_m) = \text{rect}\left[\frac{\hat{t} - 2r_0(t_m)/c}{\tau}\right] \sigma_o \exp\{j\pi[2f_0 \frac{-2r_0(t_m)}{c} + \mu(\hat{t} - \frac{2r_0(t_m)}{c})^2]\} \quad (8)$$

where,  $r_0(t_m) = R_0(t_m) + x_0 \cos \theta_m + y_0 \sin \theta_m$

Let  $T_0(t_m) = \frac{2r_0(t_m)}{c}$  and the FFT of transmitted signal envelope is

$$P(\omega) = FFT_i \left\{ \text{rect} \left[ \frac{\hat{t}}{\tau} \right] \exp(j\pi\mu\hat{t}^2) \right\} \quad (9)$$

The FFT of  $s_0(\hat{t}, t_m)$  for  $\hat{t}$  is

$$X_0(\omega, t_m) = \sigma_0 \exp \left\{ -j2\pi f_0 T_0(t_m) \left( 1 + \frac{\omega}{\omega_0} \right) \right\} \cdot P(\omega) \quad (10)$$

That is

$$X_0(\omega, t_m) = \sigma_0 \exp \left\{ -j2\pi \frac{2(R_0(t_m) + x_0 \cos \theta_m + y_0 \sin \theta_m)}{\lambda} \left( 1 + \frac{\omega}{\omega_0} \right) \right\} \cdot P(\omega) \quad (11)$$

From the system response view, ISAR deceptive jamming can be seen as the output acquired by  $X_0(\omega, t_m)$  passing through the system with impulse response  $H(\omega, t_m)$  which is the expression of frequency domain of the false target system. The real target echo signal is expressed by (3) and its spectrum is  $X(\omega, t_m) = FFT_i \{s_r(\hat{t}, t_m)\}$ , ISAR echo including the deceptive jamming signal is:

$$Y(\omega, t_m) = X(\omega, t_m) + Y_0(\omega, t_m) = X(\omega, t_m) + X_0(\omega, t_m) \cdot H(\omega, t_m) \quad (12)$$

The Eqn (11) shows that ISAR image that contains both real target and the interference produced by the deceptive jamming  $Y_0(\omega, t_m)$ . If  $H(\omega, t_m)$  is designed according to the structure of false target, ISAR image will contain the deceptive component. To assure deceptive jamming imaging in ISAR image, the jamming signal should be similar to real target ISAR echo signal, so signal parameters transmitted by ISAR should be detected to acquire the same  $P(\omega)$  when  $t_m$  is different. To assure deceptive component image covering real target in the ISAR region, the power transmitted by ISAR deceptive jammer can be increased to make the real target response as weak as possible because of dynamic scope of ISAR receiver, so the real target disappears in the final ISAR image. The method for the production of false target echo signal is deduced in detail in the following.

If the location of each false target scatters relative to the jammer position is  $(\Delta x_j, \Delta y_j)$  where  $\Delta x_j = x_j - x_0$ ,  $\Delta y_j = y_j - y_0$ , just assume the frequency domain of the false target system is

$$H(\omega, t_m) = \sum_j \sigma'_j / \sigma_0 \exp \left\{ -j2\pi \frac{2(\Delta x_j \cos \theta_m + \Delta y_j \sin \theta_m)}{\lambda} \left( 1 + \frac{\omega}{\omega_0} \right) \right\} \quad (13)$$

Then the spectrum of jamming signal is

$$Y_0(\omega, t_m) = X_0(\omega, t_m) \cdot H(\omega, t_m) = \sigma_0 \exp \left\{ -j2\pi \frac{2(R_0(t_m) + x_0 \cos \theta_m + y_0 \sin \theta_m)}{\lambda} \left( 1 + \frac{\omega}{\omega_0} \right) \right\} \cdot P(\omega) \times \sum_j \sigma'_j / \sigma_0 \exp \left\{ -j2\pi \frac{2(\Delta x_j \cos \theta_m + \Delta y_j \sin \theta_m)}{\lambda} \left( 1 + \frac{\omega}{\omega_0} \right) \right\} \quad (14)$$

The simplification of the above equation is

$$Y_0(\omega, t_m) = X_0(\omega, t_m) \cdot H(\omega, t_m) = \sum_j \sigma'_j \exp \left\{ -j2\pi \frac{2(R_0(t_m) + x_j \cos \theta_m + y_j \sin \theta_m)}{\lambda} \left( 1 + \frac{\omega}{\omega_0} \right) \right\} \cdot P(\omega) \quad (15)$$

So the false target echo donated by Eqn (15) is the summation of the jamming signal of each scatter  $(x_j, y_j)$ . For shortly, the basic process of ISAR deceptive jamming is to acquire the ISAR working parameters of transmitted signal, the locations and intensity of false target scatters first, and determine false target system response function  $H(\omega, t_m)$  as the Eqn (13). These impulse response functions are formed and stored by jammer, and the ISAR signal spectrum  $X_0(\omega, t_m)$  is acquired by under-mixed-frequency and FFT of the transmitted signal received by the jammer, the IFFT of multiplication of  $X_0(\omega, t_m)$  and the stored response functions  $H(\omega, t_m)$  at each  $t_m$  is just the jamming signal which will be transmitted back to ISAR by up-mixed-frequency.

### 3. PRINCIPLE OF ISAR ANTI-JAMMING BASED ON SLOPE-VARYING LFM SIGNAL

It can be seen from Section 2 that to synthesis the jamming signal, deceptive jammer should detect radar transmitted signals, analyse the signal parameters, and store its phase. Generally speaking, the side subjected to interference can acquire the way by which the signal is produced with the cheating and other method, and then the relation between the jamming signal and radar transmitted pulse signal is acquired, so it can be considered that ISAR anti-deceptive jamming would be realised by some signal agile technology. For ISAR imaging process, the compression of scatters cross-range signal along azimuth direction makes the frequency agility in slow-time domain unusable, so only modulation of some signal parameters agility in fast-time domain can be considered. Soumekh[6], *et al.* have proposed the signal agile technology such as amplitude modulation, random jump of the initial phase, and slope-varying of LFM signal when doing research in anti-jamming against SAR. The simulation result has shown that the former two agile technologies are poor in the improvement of deceptive anti-jamming performance [6]. So studies were carried out on signal agile technology based on slope-varying in derail, and apply it to ISAR deceptive anti-jamming for the first time in our research. Firstly, in the case of dechirp process widely used in ISAR imaging, the difference of pulse compression gain at range direction between the real and the false targets after slope-varying was analysed; Secondly, for the change of signal bandwidth and range resolution after slope-varying, the interpolation at range direction before the process at azimuth direction has been proposed, and the method of Doppler domain averaging was adopted by which part of the phase error induced by interpolation was removed and the real target ISAR image was improved.

#### 3.1 Analysis of Dechirp Process Gain of Real and False Scatters Echo

If ISAR transmits LFM signal with slope  $\mu$  at the  $t_m$  moment, the echo signal of scatters at the distance  $R_i(t_m)$  is

$$s_{REAL}(\hat{t}, t_m) = \sigma \text{rect} \left[ \frac{\hat{t} - 2R_i(t_m)/c}{\tau} \right] \exp \left\{ j\pi \left[ 2f_0 \left( t - \frac{2R_i(t_m)}{c} \right) + \mu \left( \hat{t} - \frac{2R_i(t_m)}{c} \right)^2 \right] \right\} \quad (16)$$

If the delayed signal with slope  $\mu$  at the distance  $R_{ref}$  is selected as reference signal:

$$s_{ref}(\hat{t}, t_m) = \sigma \text{rect}\left[\frac{\hat{t} - 2R_0/c}{\tau}\right] \exp\{j\pi[2f_0(t - \frac{2R_0}{c}) + \mu(\hat{t} - \frac{2R_0}{c})^2]\} \quad (17)$$

The mixed-frequency result of  $s_{ref}(\hat{t}, t_m)$  and  $s_{REAL}(\hat{t}, t_m)$  is

$$s_{y-REAL}(\hat{t}, t_m) = \sigma \text{rect}\left[\frac{\hat{t} - 2R_i(t_m)/c}{\tau}\right] \exp[-j\frac{4\pi\mu}{c}(\hat{t} - \frac{2R_{ref}}{c})R_\Delta(t_m)] \exp[-j\frac{4\pi}{c}f_0R_\Delta(t_m)] \exp[j\frac{4\pi\mu}{c^2}R_\Delta^2(t_m)] \quad (18)$$

where  $R_\Delta(t_m) = R_i(t_m) - R_{ref}$ . It can be seen from the Eqn (18) that the FFT about  $\hat{t}$  is the range profile of real target, and the real scatter with form a peak with intensity  $\sigma\tau$  at  $-\frac{2R_\Delta(t_m)\mu}{c}$  in frequency domian.

If the jammer still produces jamming signal according to the slope  $\mu_0$  of the detected LFM signal at  $t_m$  moment, the echo signal of false scatters at the distance  $R_j(t_m)$  is:

$$s_{FALSE}(\hat{t}, t_m) = \sigma \text{rect}\left[\frac{\hat{t} - 2R_j(t_m)/c}{\tau}\right] \exp\{j\pi[2f_0(t - \frac{2R_j(t_m)}{c}) + \mu_0(\hat{t} - \frac{2R_j(t_m)}{c})^2]\} \quad (19)$$

ISAR dechirp process of false scatters echo still uses  $s_{ref}(\hat{t}, t_m)$  as the reference signal, the mixed-frequency of  $s_{ref}(\hat{t}, t_m)$  and  $s_{FALSE}(\hat{t}, t_m)$  is:

$$s_{y-FALSE}(\hat{t}, t_m) = \sigma \text{rect}\left[\frac{\hat{t} - 2R_i(t_m)/c}{\tau}\right] \exp[-j2\pi\frac{2f_0R_\Delta(t_m)}{c}] \exp\{j2\pi[\frac{1}{2}\mu_\Delta\hat{t}^2 - (\frac{2R_\Delta(t_m)\mu}{c} + \frac{2R_0\mu_\Delta}{c})\hat{t} + (\frac{2\mu R_i^2(t_m)}{c^2} - \frac{2\mu_0 R_0^2}{c^2})]\} \quad (20)$$

where  $\mu_\Delta = \mu - \mu_0$ , the second phase item of Eqn (20) shows that after the mixed-frequency, the false scatters echo is a LFM signal with the slope  $\mu_\Delta$  and central frequency  $-\frac{2R_\Delta(t_m)\mu}{c} + \frac{2R_0\mu_\Delta}{c}$ . The effect of each phase item to ISAR imaging is analysed in the following way.

- **Constant item**  $\frac{2\mu R_i^2(t_m)}{c^2} - \frac{2\mu_0 R_0^2}{c^2}$ : this is unique in the process of dechirp, known as the remaining video phase (RVP) which is seen as constant within one of slow-time  $t_m$  and doesn't affect the range profile; but this changes with the variety of slow-time  $t_m$ , has relatively small absolute value and can be removed [2].

- **Constant item**  $\frac{2f_0R_\Delta(t_m)}{c}$ : this is seen as constant within one of slow-time  $t_m$  and doesn't affect the range profile; but  $R_\Delta(t_m)$  known as the foundation of ISAR imaging at azimuth direction, changes with the slow-time  $t_m$  and produces Doppler frequency. Specially, after the envelope alignment and initial phase compensation, if  $R_{ref} = r_0(t_m)$ ,  $R_\Delta(t_m) = R_i(t_m) - R_{ref} = x + y\Omega t_m$  will vary with slow-time  $t_m$  linearly.

- **Linear phase item**  $-\frac{2R_\Delta(t_m)\mu}{c} + \frac{2R_0\mu_\Delta}{c}\hat{t}$ : this item produces the location error of false scatters' high resolution range profile (HRRP), with offset  $\Delta_m = \frac{R_0\mu_\Delta}{\mu}$ . The envelope of HRRP can not be aligned due to this offset. Azimuth direction

imaging defocuses and the gain of false scatters will also be reduced.

- **Quadratic phase item**  $\frac{1}{2}\mu_\Delta\hat{t}^2$ : this item reduces the intensity and broadens the main lobe of each false scatters, so the suppression of false target energy is realised. According to the spectrum characteristics of LFM signal, the bandwidth is  $B_\Delta = \mu_\Delta\tau$ . The FFT of Eqn (20) is the HRRP of false target, with the false scatter intensity  $\sigma\sqrt{\frac{\tau}{B_\Delta}}$  and broadened size  $\Delta_s = \frac{2\tau\mu_\Delta}{c\mu}$ ; the intensity of real target is still  $\sigma\tau$  through dechirp process, so after slope-varying, the suppression ratio of intensity gains about false scatters is:

$$\gamma = \sigma\tau / \sigma\sqrt{\frac{\tau}{B_\Delta}} = \sqrt{B_\Delta\tau} \quad (21)$$

The total received echo is

$$s_{echo}(\hat{t}, t_m) = s_{REAL}(\hat{t}, t_m) + s_{FALSE}(\hat{t}, t_m)$$

and the HRRP after dechirp at the  $t_m$  moment is

$$s(r, t_m) = FFT_i\{s_{echo}(\hat{t}, t_m) * s_{ref}^*(\hat{t}, t_m)\} = FFT_i\{s_{REAL}(\hat{t}, t_m) * s_{ref}^*(\hat{t}, t_m)\} + FFT_i\{s_{FALSE}(\hat{t}, t_m) * s_{ref}^*(\hat{t}, t_m)\} \quad (22)$$

It can be seen from the above that the relative change of slope is larger, the bandwidth of false echo signal is wider, the peak of scatter is much lower, and the spread of main lobe is more obvious, so the suppression of false scatters is much greater. Figure 2 shows the comparison between real and false scatters energy gain through dechirp process respectively while the transmitted signal has the bandwidth 100  $\mu$ s, pulse duration and ration of slope-varying  $\mu_\Delta/\mu = 1\%$ . Because of the slope-varying, the fixed frequency modulation slope of false target echo is mis-matched, the gain decreases by 30dB, and the suppression of false target is realised.

Figure 3 shows the relationship between gain suppression and ratio of slope-varying which indicates that when the

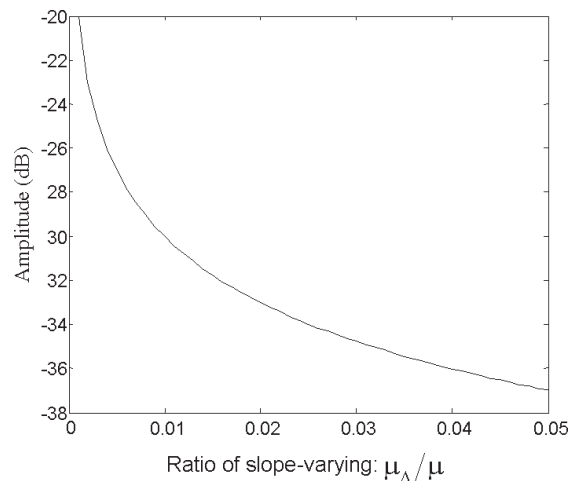
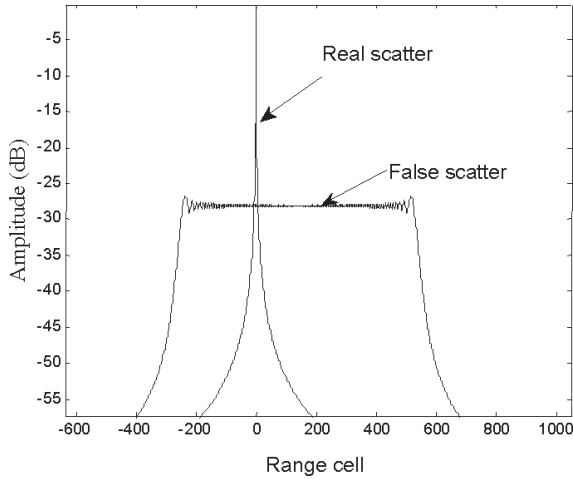


Figure 2. Comparison of the dechirp gain about real and false scatters' echo with slope-varying.



**Figure 3. Relation of the ratio of slope-varying and gain suppression.**

ratio of slope-varying is much larger than 3%, the decline of gain suppression is less obvious. Of course, the slope variety of LFM signal can not be too large, according to the requirement of suppression ratio and radar parameters, and the ratio of slope-varying can be calculated by Eqn (21).

### 3.2 Improvement of ISAR Imaging by Doppler Domain Averaging

Assume that the pulse duration of radar transmitted signal is unchanged, the slope-varying will induce the change of signal effective bandwidth ( $B = \mu\tau$ ) and range resolution  $\rho_r = c/2B$ . Given the range resolution  $\rho_{r0} = c/2\tau\mu_0$  corresponding to slope  $\mu_0$ , then  $\rho_r = \rho_{r0} / (1 + \frac{\mu_\Delta}{\mu_0})$ , the HRRP of  $s_{echo}(\hat{t}, t_m)$  is acquired by discrete sampling with the sample frequency  $f_s$  and sampling points is  $N = \tau f_s$ , after mixed-frequency and FFT transform, each sampling point corresponds to range  $r_n = (n - N/2)\rho_r$ ,  $i = 0, 1, \dots, N-1$ . Because of different varying slope inducing various range resolution of HRRP  $s(r, t_m)$  at each  $t_m$  moment, the energy of scatters still disperse among adjacent range cells after envelope alignment, so the direct FFT along azimuth direction will inevitably lead to defocus. The method proposed in this paper is that  $M$  slow-time series of HRRP  $s'(r, t_m)$  with the same range resolution  $\rho_{r0}$  is acquired by range interpolation for eachs ( $r, t_m$ ), and after envelope alignment and initial phase correction, the FFT at azimuth direction will produce ISAR image. It is unfortunately that the range interpolation will result in some phase error of each range cell of  $s'(r, t_m)$  and Doppler blurring along azimuth direction in final ISAR image. In this paper, a simple, feasible and relatively low time-consuming method of Doppler domain averaging is proposed to remove the Doppler blurring produced by part of high order phase and achieve relatively much more clear ISAR image, which is already been used in SAR.[5]

After range interpolation, a scatter signal is

$$s'(r_n, t_m) = \sigma \exp[j \frac{4\pi f_0}{c} R_\Delta(t_m)] \text{ in the } n\text{-th range cell.}$$

The range interpolation changes  $R_\Delta(t_m)$  and the phases of signal are contaminated consequently.

Suppose  $R_\Delta(t_m) = \sum_{n=0}^{\infty} \frac{1}{n!} R_\Delta^{(n)} t^n$ , the FFT of  $s'(r_n, t_m)$  is

$$\begin{aligned} s'(r_n, \omega) &= \sigma \int \exp[j \frac{4\pi f_0}{c} \sum_{n=0}^{\infty} \frac{1}{n!} R_\Delta^{(n)} t^n] \cdot \exp(j\omega t) dt \\ &= \sigma e^{j \frac{4\pi f_0 R_\Delta^{(0)}}{c}} \delta(\omega - \frac{4\pi f_0 R_\Delta^{(1)}}{c}) \otimes_\omega FFT\{\exp[j \frac{4\pi f_0}{c} \sum_{n=2}^{\infty} \frac{1}{n!} R_\Delta^{(n)} t^n]\} \end{aligned} \quad (23)$$

where,  $R_\Delta^{(n)}$  is the  $n$ th derivative of  $R_\Delta(t_m)$  at  $t_m = 0$ ,  $R_\Delta^{(1)}$  is related to scatter location along azimuth direction, but because of range interpolation,  $R_\Delta(t_m)$  has quadratic or high order phase with  $t_m$  which induce the Doppler ambiguity at  $\omega = \frac{4\pi f_0 R_\Delta^{(1)}}{c}$ . The average of  $s'(r_n, \omega)$  along azimuth direction is

$$\begin{aligned} E(r_n, \omega) &= \frac{1}{2\pi} \int s'(r_n, \omega + \phi) s'^*(r_n, \omega - \phi) d\phi \\ &= \frac{\sigma^2}{2\pi} \iiint \exp[j \frac{4\pi f_0}{c} \sum_{n=0}^{\infty} \frac{1}{n!} R_\Delta^{(n)} t^n] \cdot \exp(j(\omega + \phi)t_1) \cdot \\ &\quad \exp[-j \frac{4\pi f_0}{c} \sum_{n=0}^{\infty} \frac{1}{n!} R_\Delta^{(n)} t^n] \cdot \exp(-j(\omega - \phi)t_2) dt_1 dt_2 d\phi \end{aligned} \quad (24)$$

The Eqn (24) is simplified by  $\int \exp(j\phi(t_1 + t_2)) d\phi = 2\pi\delta(t_1 + t_2)$ :

$$\begin{aligned} E(r_n, \omega) &= \sigma^2 e^{j \frac{8\pi f_0 R_\Delta^{(0)}}{c}} \delta(\omega - \frac{4\pi f_0 R_\Delta^{(1)}}{c}) \otimes_\omega \\ &\quad FFT\{\exp[-j \frac{4\pi f_0}{c} \sum_{n=1}^{\infty} \frac{1}{(2n+1)!} R_\Delta^{(2n+1)} t^{2n+1}]\} \end{aligned} \quad (25)$$

It can be seen from the above that the Doppler ambiguity induced by  $E(r_n, \omega)$  is related to the third and higher odd-order phase, and the effect of second and higher even-order phase is removed. The discrete Eqn (24) is

$$E(r_n, \omega_m) = \frac{1}{2L} \sum_{i=-L}^L s'(r_n, \omega_{m+i}) \cdot s'^*(r_n, \omega_{m-i}) \quad (26)$$

### 3.3 ISAR Anti-Jamming Working Flow Based on Slope-Varying

For short, the process flow of ISAR active anti-deceptive jamming based on slope-varying technology is described as follows:

- (i) To avoid slope-varying detected by the jamming side, the set of varying frequency modulation slope  $\Gamma = \{\mu_1, \dots, \mu_Q\}$  can be specified before ISAR imaging.
- (ii) At each slow-time  $t_m$  the slope parameter  $\mu_m$  of transmitted signal  $s_t(\hat{t}, t_m)$  is randomly selected from  $\Gamma$  so as to make it more difficult for effective jamming.
- (iii) Construct reference signal  $s_{ref}(\hat{t}, t_m)$  for each echo  $s_{echo}(\hat{t}, t_m)$  at the  $m$ -th pulse repetition period, and after dechirp process the range profile of real target is obtained and the energy of false target is suppressed. Then coarse target ISAR image will be produced by FFT transform along azimuth direction.

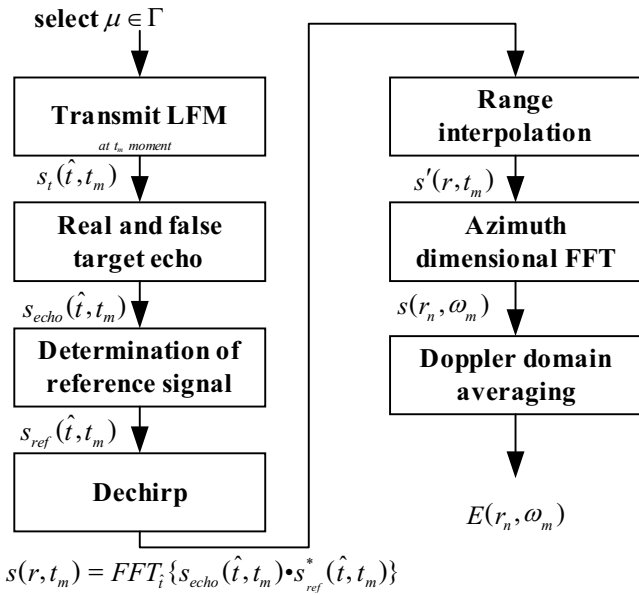


Figure 4. Flow of ISAR deceptive anti-jamming based on slope-varying.

(iv) Doppler domain averaging is used for improving the quality of the coarse ISAR image.

4. SIMULATIONS

The following parameters of radar are set up for later simulations: transmits LFM signal with the carrier frequency 10GHz, effective bandwidth 0.4GHz, PRF 0.5KHz, and pulse duration 40μs.

The simulation is carried out on a computer with 2.5 GHz CPU and 1.25 Gb RAM, and the software tool which is applied here for programming is Matlab 7.0. For application of this technique in practice, there is no other additional time consuming besides Doppler domain averaging operation compared with normal ISAR processing. But it is really complicated modification for radar transmitter and receiver's hardware which is not taken into account in this paper.

4.1 Result of Simulation in the Case of Separated Real and False Targets

The real and false targets are located among the same range window but are separate from each other along azimuth direction, which cheats ISAR of several false targets being in radar image. Assume that the real target consists of four scatters with the square shape, their locations are (10,7.5), (10,5.5), (5,7.5), (5,5.5), the false target also consists of our scatters with the location (-4,-4), (-6,-8), (-4,-8), (-6,-4), the intensity of each scatter is set to be 1, the relative rotation angle of target is 3°, the pulse number of coherent integration is 512. If LFM signal with the same slope transmitted by radar is detected by the jamming side and the jammer simulates the false target echo, the ISAR image containing all of targets is shown in Fig. 5. If the radar transmits LFM signal with the slope-varying, the jammer still simulates the false target echo according to the detected LFM signal parameter

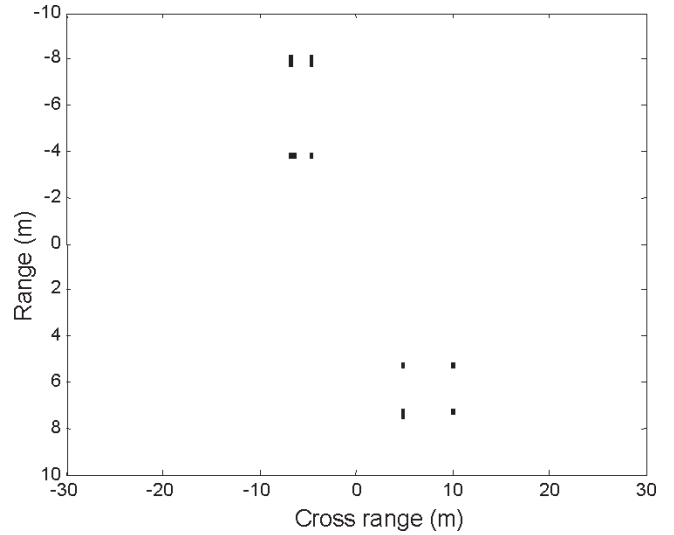


Figure 5. ISAR image of real and false targets' echo with no slope-varying

μ<sub>0</sub>, and the ISAR image is shown in Fig. 7. Figure 6 shows the previous 50 pulses' ratio of slope-varying μ<sub>Δ</sub>/μ<sub>0</sub> corresponding to each slow-time. It can be seen from Fig. 7 that most of false target energy is suppressed, but the range interpolation induces a little Doppler ambiguity along azimuth direction, ISAR image processed by the Doppler domain averaging in the section 3.2 is shown in Fig. 8, here the energy of false points is removed mainly and real target ISAR image is much clearer. And by using the computer environment described above, the time of Doppler domain averaging operation is about 563 ms which can be further reduced by FPGA in real hardware configuration.

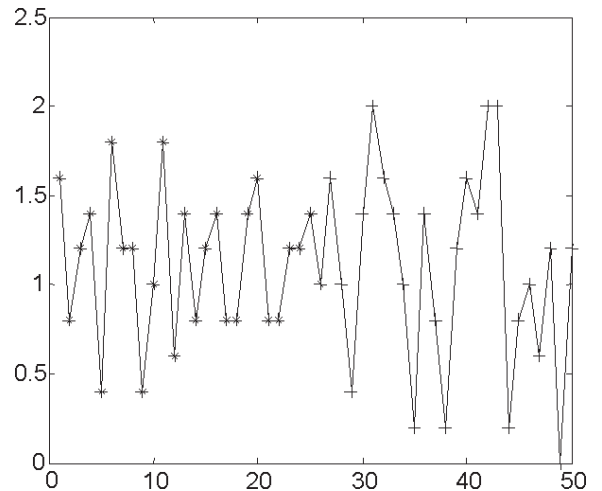


Figure 6. Ratio of each pulse's slope-varying.

4.2 Result of Simulation in Overlapped Real and False Targets

The real and false targets are located among the same range window but overlap with each other, which makes ISAR image fuzzy and target recognition difficult. The real target consists of several scatters similar to the structure of aircraft, and the false

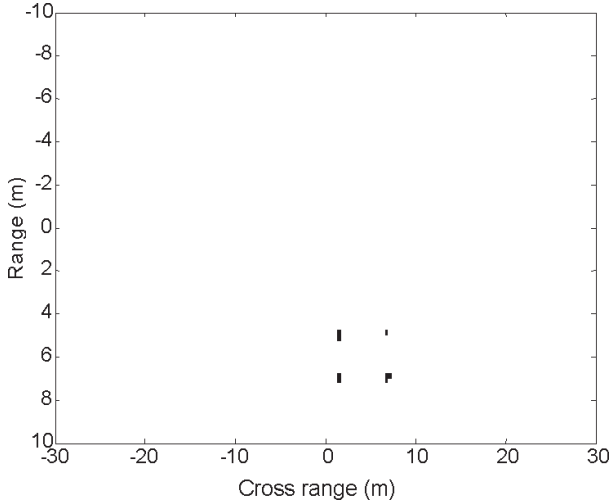


Figure 7. ISAR image of real and false targets' echo with slope-varying.

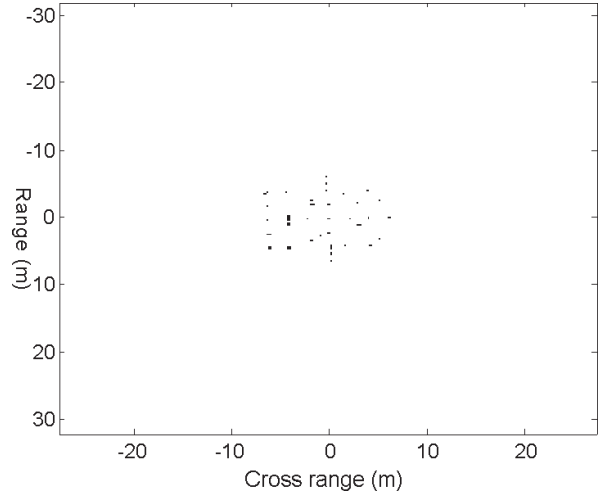


Figure 9. ISAR image of real and false targets' echo with no slope-varying.

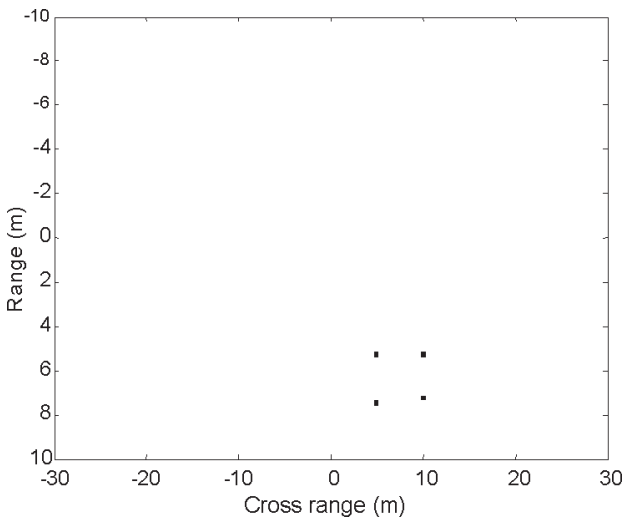


Figure 8. ISAR image of real target after Doppler domain averaging.

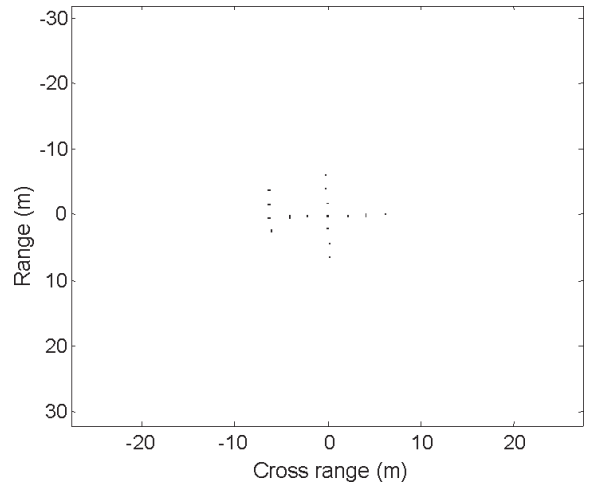


Figure 10. ISAR image of real target after Doppler domain averaging.

target consists of several scatters which spread around the real target, given the same intensity of all the scatters. Figures 9 and 10 are the ISAR images with and without slope-varying, respectively, it can be seen that the method proposed in this paper suppresses the energy of false target preferably.

### 4.3. Comparison with other LFM Phase Modulation Technique

Phase-modulation is a popular scheme for LFM pulse diversity[6] in which  $s_i(\hat{t}, t_m)$ 's rectangle envelope  $rect[\frac{t-mT}{\tau}]$  is substituted by an amplitude signal  $a(t)$  with a slowly fluctuating phase function.

$$a(t_m) = \exp[j\phi_m(t)] \quad (27)$$

To prevent the jammer from estimating this amplitude signal  $a(t)$  from multiple radar pulses, the ISAR should alter the amplitude signal  $a(t)$  at each pulse transmission. This will confuse the jammer and the cheating is disabled. But unfortunately, the PSF (Point Spread Function) of the

range imaging is as following via dechirp processing[7]

$$PSF_\omega(\omega) = FFT_t\{a^*(t)\} \quad (28)$$

So phase-modulation with  $a(t)$  above will make degradations in the PSF of range imaging via dechirp processing. For instance, the phase modulation  $\phi_m(t)$  is commonly defined by

$$\phi_m(t) = \sum_{n=1}^{N_a} a_{mn} \cos(\omega_{mn}t + \theta_{mn}) \quad (29)$$

where  $a_{mn}$  and  $\theta_{mn}$  are generated randomly which is known to ISAR,  $N_a$  is the number of harmonics. Figure 11 shows comparison between the range imaging (PSF) of an idea scatter after phase-modulation with amplitude signal  $a(t)$  and slope-varying. It is obvious that the peak of PSF is much lower and the width of PSF is much spread. As the number of harmonics is increased, the PSF of the range imaging via dechirp exhibits more undesirable side lobes, spreading, and peak power reduction. So slope-varying is a more feasible and reasonable approach for countering ISAR deceptive jamming.

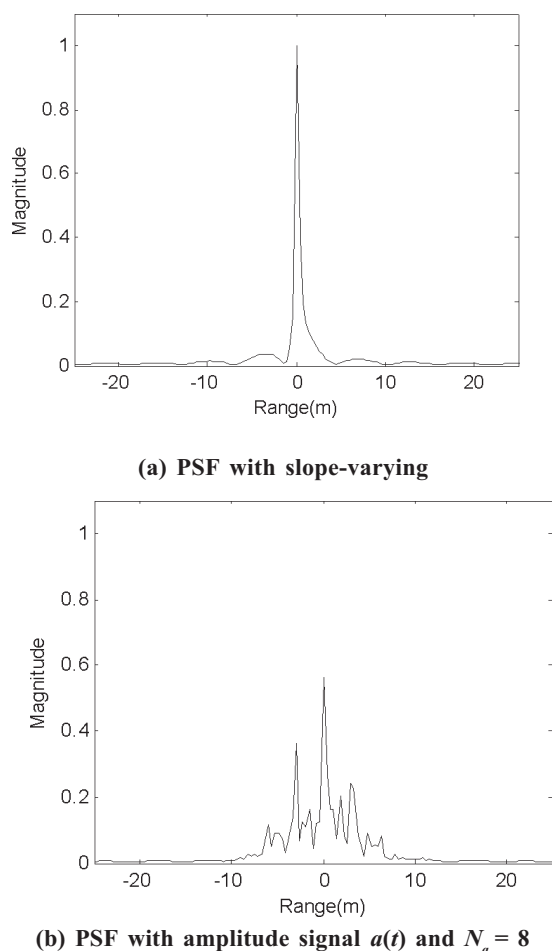


Figure 11. ISAR image of real and false targets' echo with no slope-varying.

## 5. CONCLUSIONS

At present, the technologies of DIS and DFRM can realise ISAR deceptive jamming, simulate the false target signal, and disturb the accurate target perception and recognition. To improve the ECCM performance of ISAR in the battlefield, it is necessary to study the new technology of ISAR anti-deceptive jamming. Based on the detailed analysis of the principle of ISAR deceptive jamming, this paper proposes a new technology of ISAR anti-deceptive jamming based on slope-varying, acquires the relation between the suppression of false target energy and the ratio of slope-varying. At the same time, to solve the problem of azimuth Doppler blurring induced by range interpolation, Doppler domain averaging for improvement of ISAR image is put forward here, the method has been verified to be effective and potential by simulation. Of course, the technology of slope-varying requires adjustment for radar system, which will make it challenging for practical applications.

## REFERENCES

1. Vignaud, Luc. Inverse synthetic aperture radar imaging of satellite. *Int. J. Imaging Syst. Technical*, 1998, **9**, 24-28.
2. Zheng, Baq; Mengdao, Xing & Wang, Tong. Radar imaging technology. Beijing: the Press of Electronic Industry, 2005.(In chinese)
3. Pace, P.E.; Fouts, D.J. & Ekestorm, S. Digital false-target image synthesiser for countering ISAR. *IEE Proc on Radar Sonar Navig.*, 2006, **149**(5), 248-57.
4. Fei An & Xiaojian Xu. Real-time ISAR image synthesis of ballistic targets. *In IEEE International Symposium on Microwave, Antenna, Propagation and EMC Technologies for Wireless Communications Proceedings*, 2005. pp 326-29.
5. Popovi'c, Vesna; Dakovi'c, Miloš; Thayaparan, Thayanathan & Stankovi'c, LJubiša. SAR image improvements by using the S-method. *ICASSP Proceedings*, 2006, 177-80.
6. Soumekh, Mehrdad & Narayanan, R.M. SAR-ECCM using phase-perturbed LFM chirp signals and DFRM repeat jammer penalization. *In IEEE Radar Conference*, 2005. pp 507-12.
7. Soumekh, Mehrdad. Synthetic aperture radar signal processing with matlab algorithms. New York, Wiley, 1999.

## Contributors

**Mr Zhu Yupeng** obtained his MS degree in electrical engineering in 2004 from National University of Defense Technology, Changsha, China, where he is currently working toward the PhD degree in information and communication engineering. His research interests include non-linear signal processing, radar imaging, pattern recognition, and information fusion.

**Mr Wu Liang** obtained his MS degree in electrical engineering in 2007 from National University of Defense Technology, Changsha, China, where he is currently working toward the PhD degree in information and communication engineering. His research interests include non-stationary signal processing, radar imaging, electronic jamming and anti-jamming.

**Mr Wang Hongqiang** obtained his MS degree in information engineering in 1999 and the PhD degree in information and communication engineering in 2003 from National University of Defense Technology (NUDT), Changsha, China. He is currently working as a researcher in NUDT. His research interests include radar target tracking and information fusion.

**Mr Li Xiang** graduated from Xidian University, Xi'an, China in 1993. He received the MS degree in information engineering in 1996 and the PhD degree in information and communication engineering in 1998 from NUDT, Changsha, China. He is currently working as a professor in NUDT. His research interests include radar signal processing, information fusion and radar target recognition.